

## Electron evaporation of carbon using a high density plasma.

S. Muhl

*Instituto de Investigaciones en Materiales, U.N.A.M., México, D.F., México.*

E. Camps, L. Escobar-Alarcón

*Instituto Nacional de Investigaciones Nucleares, Edo. de México, México*

O. Olea

*U.A.E.M, Edo. de México, México.*

High-density plasmas are often used either in the preparation of thin films or for the modification of surfaces; nitriding. However, except for collision-driven chemical reactions the electrons present are not used, although electron bombardment heating of the work piece nearly always occurs. Principally it is the ions and neutrals that are utilised for materials processing. By suitable biasing of a conducting source material the electrons can be extracted from a high-density low-pressure plasma to such an extent that evaporation of this source material can be achieved. Due to the presence of the plasma and the flux of electrons a large proportion of the evaporant is expected to be ionised. We have used this novel arrangement to prepare thin films of carbon using a resonant high-density argon plasma and a water cooled rod of high purity graphite. Multiple substrates were used both outside of, and immersed in, the plasma.

We report the characteristics of the plasma (electron temperature and density, the ion energy and flux, and optical emission spectra), the deposition process (the evaporation rate and ion/neutral ratio), and the film properties (IR and UV/Vis absorption spectra, Raman spectra, elemental analysis, hardness and refractive index).

### 1. Introduction

Plasma assisted physical vapour and chemical deposition (PVD & CVD) processes are used extensively in today's high technology industries and in many research labs to study the preparation of both new materials, as well as, more commonplace compounds with improved properties. The preparation of thin films of diamond-like carbon (DLC) [1] is a notable example of a material which is extremely difficult to synthesise without the use of plasmas. In fact, DLC is not one substance but a family of materials; the properties of carbon films are determined by the relative amounts of  $sp^1$ ,  $sp^2$  and  $sp^3$  bonding between the carbon atoms [2], although frequently only the  $sp^2$  and  $sp^3$  bonding configurations are considered. When the degree of  $sp^3$  bonding is low the material is amorphous carbon and has low density,  $1.6 - 2.2 \text{ gm/cm}^3$ , is soft,  $10 - 30 \text{ GPa}$ , opaque with a bandgap of  $<1.4 \text{ eV}$ , and contains little residual stress [3] signifying that there is almost no restriction on the thickness of the film that can be fabricated. Conversely, material with more than 75%  $sp^3$  bonding, which is what is normally classified as DLC, has high density,  $2.8 - 3.4 \text{ gm/cm}^3$ , is hard,  $50 - 100 \text{ GPa}$ , transparent with a bandgap of  $1.7 - 2.3 \text{ eV}$ , but the high levels of intrinsic residual stress,  $8 - 12 \text{ GPa}$ , limits the maximum film thickness to  $\sim 800 \text{ nm}$  because of adhesion failure with the substrate.

Many of the preparation methods rely on hydrogenated gaseous precursors and this results in the formation of hydrogenated amorphous carbon (a-C:H) [4,5]. The properties of such material is determined by both the type of bonding present and the hydrogen content, with the most extreme properties only occurring at relatively low concentrations of hydrogen. It is generally accepted that the transformation of part of the  $sp^2$  bonded carbon, which is the configuration which initially forms on the

surface of the deposit, to the  $sp^3$  form occurs by the densification and/or introduction of high levels of localised energy in the subsurface region of the coating. This process is caused by the incidence of fairly high level,  $>50 \text{ eV}$ , carbon species. Such species are easily generated within a plasma by the acceleration of carbon ions and, in fact, studies have shown that the formation of good quality DLC is enhanced by the use of high levels of bombardment of carbon ions relative to the number of incident carbon atoms. Additionally, low substrate temperatures are required to reduce the thermal relaxation of the densification process [6].

The principally techniques that have been used to make DLC films include; mass selected ion beam deposition (MSIBD) [7,8,9,10], RF plasma CVD [11,12,13], magnetron sputtering [14,15,16], vacuum arc PVD [17,18,19] and pulsed laser deposition [20,21,22], with substrate biasing to control the energy of the incident carbon ions. MSIBD is a highly sophisticated technique but is not readily useable as an industrial method and RFCVD can only be used to prepare a-C:H. The disadvantage of magnetron sputtering is that the plasma density is normally quite low,  $\sim 10^8 - 10^9 \text{ cm}^{-3}$ , and therefore it is difficult to get bombardment of the growing film by a high proportion

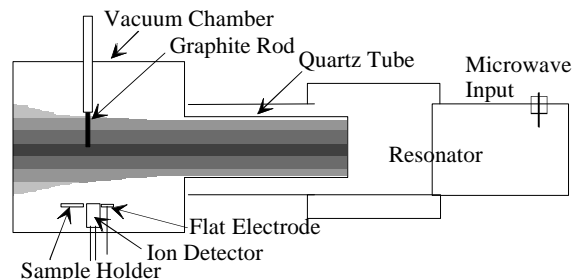


Figure 1. Schematic drawing of the ECR system.

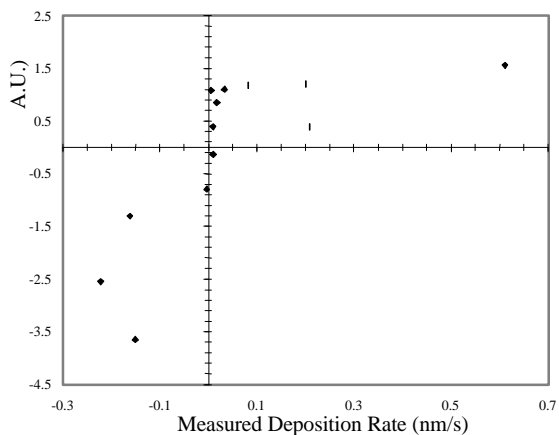


Figure 2. Graph of the calculated and observed deposition rates.

of carbon ions relative to carbon atoms. Both the arc and laser methods suffer from problems related to the inclusion of macro particles, emitted from the solid carbon source, in the deposit. However, both techniques have the advantage that only carbon species and electrons are incident on the substrate. In summary, high quality DLC films have more than 80%  $sp^3$  carbon bonding, and this is achieved using low substrate temperatures and growth, principally, by carbon ions which have energies in a range from 60 to 200eV.

**2. Experiment**

Electrons extracted from an intense low pressure ECR argon plasma were used to thermally evaporate carbon from a biased graphite rod. The intense electron flux causes almost complete ionisation of the emitted carbon atoms and a combination of the plasma conditions and the bias controls the energy of the carbon ions. The details of the ECR equipment have been published elsewhere [23] but basically the ECR condition is established in one section of the apparatus and a high-density plasma beam, approximately 6cm. diameter, is directed into the deposition chamber by a magnetic field gradient generated by three electromagnetic coils. The water-cooled and biased graphite rod was placed horizontally and perpendicular to this plasma beam, as shown in the figure 1. The optimum lateral position of the rod depends on the plasma conditions as well as the electron current and ion energy required for a given experiment. Indeed, the rod position and length are additional experimental control parameters. Carbon is emitted from the end of the rod in a almost spherical distribution, when it is deeply immersed within the plasma, and with a more forward facing cone shaped distribution when the rod is placed at the edge of the plasma. The substrates were placed in front of, and in line with, the axis of the graphite rod, again as shown in the figure 1. In this position, outside the plasma, there is little electron bombardment of the substrate.

Experiments have been performed using argon and helium plasmas at  $4 \times 10^{-4}$  Torr, a microwave power of

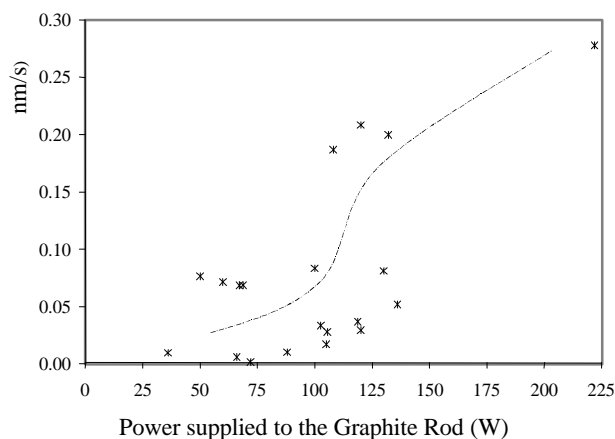


Figure 3. Graph of the deposition rate versus the electrical power supplied to the graphite rod. The line is a guide to the eye.

320W, for various rod positions and lengths, with bias voltages of the graphite rod,  $V_{graf}$  300 – 600V, and adjustment of the magnetic fields to control the current in the graphite rod,  $I_{graf}$ .

The plasma characteristics were measured using an electrostatic probe and the ion energy,  $I_E$ , and flux,  $I_F$ , were determined using a Faraday cup analyser with an electron expelling electrode and a variable ion retarding potential. Additionally, some experiments were carried out using a 2.6cm. diam. flat copper electrode placed near the ion detector. Analysis of the I/V characteristic of this electrode permitted an evaluation of the floating potential of the substrates. We were able to find the effective area of the entrance to the ion detector by comparing the current flowing to the flat electrode,  $I_s$ , and that seen by the ion detector,  $I_d$ [24]. The films were prepared on cleaned 1cm. x 1cm. pieces of (100) silicon wafers and Corning 7059 borosilicate glass. Substrates were either placed on an electrically floating holder or on the biased flat electrode using silver paste. In this way deposits could be grown simultaneously at the floating potential of the plasma,  $V_f$ , or at the voltage applied to the electrode,  $V_{probe}$ . The deposits were characterised by ellipsometry to obtain the thickness and refractive index. The bandgap was calculated from the absorption spectra obtained using a UV-Vis spectrophotometer, and a perfilometer, Sloan Dektak IIA, was used to measure the thickness and residual stress through the application of the beam bending technique. The film resistivities were measured by standard techniques using two silver dag electrodes, 0.8 x 0.2cm with a separation of 0.1cm. SEM and EDAX were employed to determine the film topography and impurity content.

**3. Results**

Using argon it was relatively easy to obtain sufficient plasma density to be able to evaporate the carbon, however high values of biasing of the graphite resulted in a strong perturbation of the plasma. The energy of the ions incident on the substrate could be controlled by varying  $V_{graf}$  when the ion current was at a high value, but for moderate ion

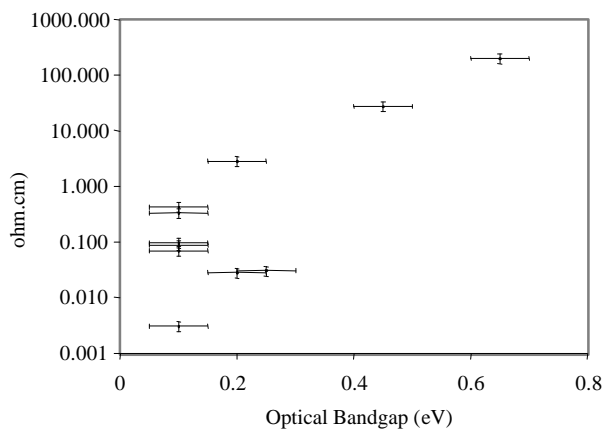


Figure 4. The film resistivity versus the measured optical bandgap.

currents the ion energy was mainly dependent on the plasma parameters. Using the present experimental setup it is not possible to determine the relative proportion of argon and carbon ions. However, it was observed that under conditions of low carbon evaporation rates and high ion energies the silicon and glass substrates were sputter etched. Therefore the measured deposition rate depends on the carbon arrival rate and the sputter etch rate. We have calculated an effective deposition rate using the assumptions that the carbon arrival rate is proportional to the ion current and that the etch rate is proportional to the product of the  $I_E$  and the  $I_F$ . Figure 2 presents the observed deposition rate versus the rate estimated from the calculated arrival and etch rates using a sputtering threshold energy of  $\sim 10\text{eV}$  and a sputtering yield of  $\sim 0.02$  atoms per incident ion [26]. A considerable amount of scatter is seen, in part because of the simplified simulation and also because the proportion of carbon ions contributing to the ion current is not known. Even with this a general trend in agreement with the process model can be seen.

The carbon arrival rate, and therefore the deposition rate, is expected to be determined by the temperature of the graphite rod which, in turn, is controlled by the electrical power supplied to the graphite. Figure 3 shows a plot of the deposition rate versus this power for a large variety of plasma conditions and includes data from both the argon and helium work. Although again there is considerable scatter in the data a general trend of an increasing deposition rate with increased power can be observed.

The experiments using helium permitted the deposition of carbon films without the problems of high sputter erosion. However, the dependence of the ion energy and flux on the experimental conditions was very different to the argon case. Almost no change in the ion energy distribution spectra was observed with and without biasing of the graphite, even under conditions which made the rod white hot and an accompanying high degree of evaporation.

Additionally, with helium it was found to be more difficult to establish a sufficiently high plasma density to easily evaporate the graphite. It was possible to achieve the necessary density at pressures  $\sim 2 \times 10^{-4}\text{Torr}$ , but this

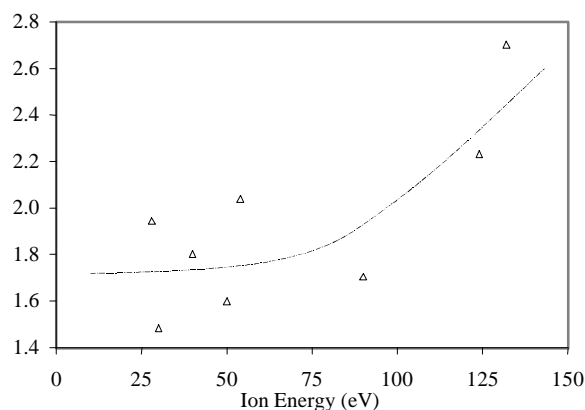


Figure 5. The refractive index of the film versus the measured ion energy. The line is a guide to the eye.

resulted in excessive heating, and failure, of the quartz tube resonator. We are at present designing and implementing modifications to the system to avoid this problem. Deposits were prepared using helium for either short times or under pulsed conditions, however the controllability of these experiments was difficult.

The figure 4 shows the variation of the resistivity and optical bandgap of the films prepared using both Ar and He, and figure 5 the variation of the refractive index of the films against the measured ion energy in helium. As is normally observed for carbon films, the bandgap increases as the resistivity rises, and the refractive index tends to be high for higher energy deposition processes.

The figure 6 shows a microscopy image of the surface of a typical film, as can be seen the surface is extreme smooth. The particle in the upper part of the micrograph was not part of the deposit but was a defect from insufficient substrate cleaning prior to deposition. The EDX elemental analysis of the films showed only the presence of carbon. In general, the films were hard in that they would resist scratching with the point of metal tweezers. In the near future the results of nanoindentation measurements will be reported. Measurement of the curvature of silicon substrates before and after deposition, using of Stoney's equation, indicated that the stress in the films varied from 0.13 to 0.66 Mpa as the ion energy increased from 40 to 100eV. Using He the measured stress was under some conditions negative. This somewhat surprising result, given the larger bandgaps and refractive indices of these films, requires further work.

#### 4. Discussion

It can be expected that the energy of the ions, that are incident on the substrate, is controlled by a combination of the voltage applied to the graphite rod and the values of the magnetic fields. The acceleration of the ions is mainly caused by the electric field between the surface of the graphite rod and the surrounding plasma, with this operating over approximately one sheath length around the rod. The sheath length ( $l_s$ ), can be found from the two expression for the current limited by space charge, between

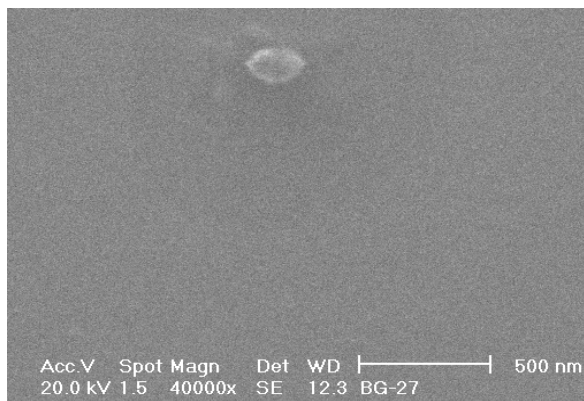


Figure 6. A high magnification SEM micrograph of a typical sample.

coaxial cylinders:

$$i = \frac{2 \sqrt{2}}{9} \sqrt{\frac{e}{m}} \frac{V_s^{3/2}}{(r b^2)}$$

Here  $i$  is the electron current per unit length,  $V_s$  the potential of the graphite with respect to the edge of the plasma sheath,  $r$  is the radius of the graphite,  $\beta=f(r/r_0)$ , where  $r_0$  is the radius of the sheath, and

$$V_{graf} = V_p + V_s$$

Where  $V_p$  is the plasma potential and  $V_{graf}$  is the applied voltage to the graphite. The calculation of  $\beta$  is quite complicated, see ref. [25], but basically the value of  $r_0$  is inversely proportional to the density of the plasma.

Changes in the plasma parameters cause corresponding changes in  $r_0$  and  $V_s$ , and these determine the electric field and the energy of the ions. Since, the electric field is the product of the potential difference and the sheath length.

The carbon emission rate, and therefore the deposition rate, is controlled by the temperature of the graphite rod, and this, in turn, is determined by the energy deposited by the impacting electrons from the plasma. This energy is the product of the number of electrons that are incident and the energy of each electron. The number of electrons depends on the plasma density and the electron energy depends on the same electric field that accelerates the ions. However, the power dissipated in the graphite, it's temperature and therefore the deposition rate, can be determined from the product of the current and voltage applied to the graphite.

Therefore, it should be possible to establish, over a extensive range, plasma conditions which allow experiments with either constant deposition rates as a function of ion energy (varying  $V_{appl}$  but maintaining constant  $V_{appl} \times I_{graf}$ ), or constant ion energy as a function of the deposition rate (maintaining  $V_{appl}$  constant and varying  $I_{graf}$ ).

Additionally, if we assume that the electric field that accelerates the carbon ions emitted from the graphite rod also accelerates the plasma gas ions present in the plasma, then

$$F = Ee \quad v = u + at \quad F = ma$$

and supposing  $u = 0$  then  $mv = Ft = Eet$ .

Then the ratio of the kinetic energies,  $K_{Gas}$  and  $K_C$ , for the plasma gas and carbon ions, respectively is,

$$\frac{K_{Gas}}{K_C} = \frac{m_{Gas} v_{Gas}}{m_C v_C} \left( \frac{v_{Gas}}{v_C} \right) \quad \text{but}$$

$$\frac{m_{Gas} v_{Gas}}{m_C v_C} = 1$$

$$\text{Therefore} \quad \frac{K_{Ar}}{K_C} = \frac{v_{Gas}}{v_C} = \frac{Eet / m_{Gas}}{Eet / m_C} = \frac{m_C}{m_{Gas}}$$

For an argon plasma this results in  $K_{Ar} = 0.3K_C$  and for helium  $K_{He} = 3K_C$ . Furthermore, if  $C_2$  ions are present then their energy will be half that of  $K_C$ . Therefore, for example if the carbon ion energy is 100eV the energy of the  $C_2$ , argon and helium ions would be approximately 60, 300 and 30eV, respectively.

The process model implicitly assumes that the plasma potential is not greatly modified by the biasing of the graphite. As we have described this is essentially true for helium but not so for argon. The ion energy distribution in He was seen to be dominated by a large group of low energy ions, corresponding to their acceleration by the difference between the plasma potential and ground, and much less intense groups of ions at higher energies. The system problems referred to earlier, related to using He, did not permit a complete study of the ion energy distribution but the relative energies of the groups of ions did agree quite well with the that predicted by the model. With Ar the energy of the predominant plasma ions increased almost proportionally with the bias applied to the graphite and this inhibited the detection of groups of ions.

### 5. Conclusion

The present results do not demonstrate the formation of DLC but we believe that they do show that this novel plasma assisted process for the preparation of thin films of carbon will, with the appropriate modifications, be capable of fabricating DLC. The results indicate that the deposition of carbon accompanied by moderately intense argon ion bombardment in the range of 50 – 220eV does not lead to the formation of the  $sp^3C$  bonding configuration.

### Acknowledgements

This work was partially supported by the CONACyT projects No. 29250E and 27676E, and the project IN114998 funded by the DGAPA-UNAM.

### References

- [1] S.R.P. Silva, J. Robertson, W.I. Milne and G.A.J. Amaratunga, (edt.) "Amorphous carbon: State Of The Art", Proc. 1<sup>st</sup> Int. SMAC'97, World Scientific, Singapore (1998).
- [2] M. S. Dresselhaus and R. Kalish., "Ion Implantation in Diamond, Graphite and Related Materials".H.K.V. Lotsch

- 
- (edit.). Springer series in Materials Science, Vol. 22. 3 (1992).
- [3] J. Robertson, *Surf. and Coat. Tech.*, **50**, 185(1992).
- [4] M. Weiler, et al., *Phys. Rev. B.*, **53**, 1594(1996).
- [5] S. Sattel, J. Robertson and H. Ehrhardt, *J. Appl. Phys.*, **82**, 4566(1997).
- [6] Y. Lifshitz, G. D. Lempert and E. Grossman, *Phys. Rev. Letts.*, **72**, 2753(1994).
- [7] W. Moller, *Appl. Phys. Letts.*, **59**, 2391 (1991).
- [8] Y. Lifshitz, et al., *Diamond and Related Mats.*, **3**, 542 (1994).
- [9] E. Grossman, et al., *Appl. Phys. Letts.*, **68**, 1214(1996).
- [10] J. Kulik, et al., *J. Appl. Phys.*, **76**, 5063(1994).
- [11] G. J. Vandentop, et al., *J. Vac. Sci. Technol. A*, **9**, 2273(1991).
- [12] A. Raveh, J. E. Klemberg-Sapieha, L. Martinu and M. R. Wertheimer, *J. Vac. Sci. Technol. A*, **10**, 1723(1992).
- [13] G. J. Vandentop, et al., *Phys. Rev. B*, **41**, 3200(1990).
- [14] H. Murzin, et al., *Mat. Res. Soc. Symp. Proc.*, **498**, 153 (1998).
- [15] N. Sauvides *J. Appl. Phys.* **58**, 518(1985).
- [16] J. Schwan; et al., *J. Appl. Phys.* **79**, 1416(1996).
- [17] R. Lossy, et al., *J. Appl. Phys.*, **77**, 4750(1995).
- [18] P. J. Fallon, et al., *Phys. Rev. B*, **48**, 4777(1993).
- [19] M. Chhowalla, et al., *J. Appl. Phys.*, **81**, 139(1997).
- [20] A. A. Voevodin and M. S. Donley, *Surf. & Coat. Tech.*, **82**, 199(1996).
- [21] J. J. Cuomo, et al., *J. Vac. Sci. Technol. A*, **10**, 3414(1992).
- [22] D. Pappas, et al., *J. Appl. Phys.*, **71**, 5675(1992).
- [23] Enrique Camps, Oscar Olea, C. Gutiérrez-Tapia and Mayo Villagrán, *Rev. Sci. Instrum.*, **66**, 3219(1995).
- [24] The presence of the negatively biased electron-repulsion electrode behind the entrance aperture in this type of ion detector captures the ions that enter close to the edge of the aperture. Therefore the ion current detected is less than that which would be found from considering the physical area of the aperture. The transfer ratio of the detector is the ratio of the effective area and physical areas of the entrance.
- [25] J.L. Vossen and W. Kern (edt), *Thin Film Processes*, Cap. II., Academic Press, (1978).
- [26] I. Langmuir & K.B. Blodgett, *Phys. Rev.*, **2**, 450(1913).